JVSTA
Journal of Vacuum Science & Technology A

Spatially resolved optical emission study of sputtering in reactive plasmas

S. A. Moshkalyov, M. Machida, D. O. Campos, and A. Dulkin

Spatially resolved optical emission study of sputtering in reactive plasmas

S. A. Moshkalyov,[a] M. Machida, and D. O. Campos
Institute of Physics ''Gleb Wataghin,'' UNICAMP, C.P. 6165, 13083-970, Campinas, S.P., Brazil

A. Dulkin
Novellus Systems, M/S K-227, Palo Alto, California 94304-1025

The study of material sputtering under low-pressure reactive ion etching conditions in various gases (Cl_2, $SiCl_4$, O_2) was performed using optical emission spectroscopy with high spatial resolution. Sputtering-induced secondary photon emission (atomic and molecular) from the processed materials (Si, Al_2O_3, GaAs) was found to be strongly localized near the target surface. A spatial distribution of atomic line emission intensity was shown to be essentially nonmonotonical with distance from the surface. This effect was explained by a cascade feeding from the upper lying atomic levels, which is enhanced in plasma (collisional) environment. A simplified model accounting for the cascading has been developed, and velocities of sputtered excited atoms (in the range of $2-7 \times 10^6$ cm/s) and molecules (about $2-5 \times 10^5$ cm/s) have been evaluated from the emission spatial decay parameters. The excited sputtered atoms and molecules are produced in different types of collisions. Fast excited atoms can be produced only in the first few collisions of the incident ion in the surface top layers, whereas excited molecules are knocked off by secondary (slow) atoms originated from a collision cascade inside the solid. Based on this concept of the process, simple expressions for atomic and molecular excitation yields as functions of the incident ion flux and surface coverage were deduced. The technique can be used for *in situ* surface probing during plasma processing. © *1998 American Vacuum Society.* [S0734-2101(98)02002-8]

I. INTRODUCTION

The two major domains in a low-pressure radio-frequency (rf) discharge are the actual (bulk) plasma, where most of the gas excitation and dissociation takes place, and the plasma sheaths, the space-charge regions between the plasma and the electrodes.[1,2] In the sheath region, the positive ions produced in the plasma are accelerated towards the electrode by the sheath dc self-bias potential. Bombardment of the target surface by energetic ions is known to play an important role in plasma processing,[1,2] but the kinetics of many surface processes under ion bombardment are not yet well understood.

Optical emission spectroscopy (OES) is a useful tool for the study of reactive plasmas and plasma–surface interactions.[3,4] In OES studies, emission from the bulk plasma (plasma-induced emission) is commonly detected. However, observations of emission spectra from the sheath area (with a proper spatial resolution) can provide valuable information hardly accessible with other diagnostics. In particular, detection of spectra emitted by excited particles ejected from the target surface as a result of material sputtering by energetic ions, can give an insight into the kinetics of surface processes in the reactive plasma–surface interaction. It appears that only a small fraction ($\sim 10^{-4}-10^{-5}$) of the faster atoms produced in the first few collisions of the incident ion in the target, can leave the surface excited. These atoms have mean velocities $v > 10^6$ cm/s and represent the high-energy tail of the total sputtered flux.[5,6] The main fraction of sputtered atoms (produced in a collision cascade inside the solid) has mean velocities much less,

about $2-5 \times 10^5$ cm/s,[5,6] they leave the surface deexcited. Excited sputtered molecules may be produced only in relatively ''soft'' collisions, while in energetic collisions molecules are likely to dissociate. So, the origin of sputtering-induced optical emission appears to be essentially different for atoms and molecules.

The effect of excitation of sputtered particles was extensively investigated in beam sputtering experiments, typically performed at high ion-beam energies (~ 10 keV).[7–13] In plasma processing, much lower ion energies are applied. Probably, this is the main reason that only a few observations of sputtering-induced emission from processed materials in reactive plasmas have been reported so far.[14–17] Moreover, in many cases this emission was attributed not to direct excitation of particles during sputtering but to their subsequent excitation in plasmas.[14,17] In this study, the fluxes of sputtered excited atoms and molecules were found to be strong enough even at low discharge power, with bombarding ion energies (approximately equal to the dc self-bias potential at the powered electrode) as low as 100 eV. This indicates that in reactive plasma environments not only the sputtering yield, but also the excitation yield of sputtered particles is strongly enhanced as compared with the case of physical sputtering by nonreactive ion beams. It has been shown that whereas some properties of the secondary photon emission may be common for beam (collisionless) and plasma (collisional) environments, there are important features peculiar to the latter. In particular, in the plasma case, light emission by sputtered atoms shows essentially nonmonotonical behavior with distance from the target surface. Probably, similar effects occur in laser plums formed near a target surface during
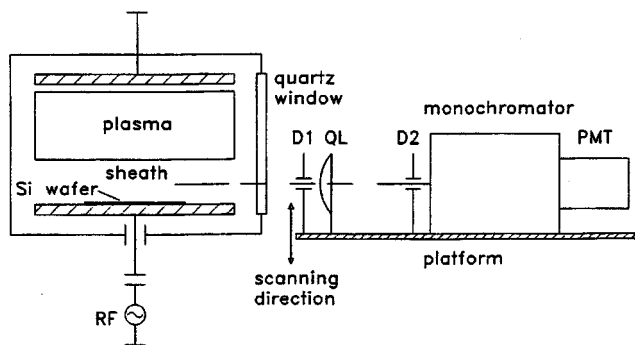
[a]Electronic mail: stanisl@ifi.unicamp.br

FIG. 1. Experimental setup. D1 and D2, horizontal slits (diaphragms); QL, quartz lens; and PMT, photomultiplier tube.

FIG. 2. Spatial distribution of emission in the sheath region, $Cl_2/Ar=6/1.5$ sccm, 125 W, 0.5 Pa, and $E_i \approx eU_{sb} \approx 900$ eV. Target: Al_2O_3 electrode+Si wafer. Sheath thickness $\approx$ 15 mm. Interelectrode gap 8 cm.

irradiation by high-fluence laser pulses, where maximum optical emission from sputtered (desorbed) target material is also observed at some distance from the surface.[18,19]

Based on the results of the study of reactive plasmas interaction with various materials (GaAs, Si, Al_2O_3), a simple model has been developed that gives the relationships between the atomic and molecular excitation yields, etch rate, and surface conditions.

II. EXPERIMENT

The schematic of the discharge chamber and diagnostic system is depicted in Fig. 1. The experimental setup is given in detail elsewhere.[20,21] A rf discharge (13.56 MHz) was run in a diode-type etcher in various gases (Cl_2/Ar, $SiCl_4/Ar$, O_2/Ar). Operational pressures, gas flow, and discharge power were varied in the ranges of 0.1–1 Pa, 3–50 sccm (standard cubic centimeters per minute), and 10–400 W, respectively. The top electrode was electrically connected with the chamber walls. In a highly asymmetric rf discharge used for reactive ion etching (RIE) processes, the dc potential difference between electrodes, ΔU_{dc}, is known to be approximately equal to the voltage drop across the sheath (i.e., the sheath self-bias potential U_{sb}) at the target (powered) electrode.[1,2] Under the present low-pressure conditions, a mean-free path for charge-transfer collisions is larger than the sheath thickness which is, typically, in the range of 1–2 cm. Thus, the measured values $\Delta U_{dc} \approx U_{sb}$ can be used to estimate roughly the maximum energies of plasma ions arriving at the powered electrode (target) surface. Hereafter, we assume the energies of ions bombarding the target surface to be equal to the self-bias potential, i.e., $E_i \approx eU_{sb}$. In most experiments, an Al_2O_3 powered electrode partly covered by a (100) Si wafer (15 and 10 cm in diameter, respectively) was utilized. In some cases, small (100) n-type GaAs samples were placed on the wafer, and the GaAs etch rate was measured after the process.

Light emission from the plasma was collected through a 10 cm diam quartz window by a quartz lens. Two horizontal slits were used for collimating of emission from a narrow area (1 mm height) parallel to the electrode. A small 0.15-m scanning monochromator (spectral resolution of about 1 nm) was employed for spectra recording in the range of 200–800
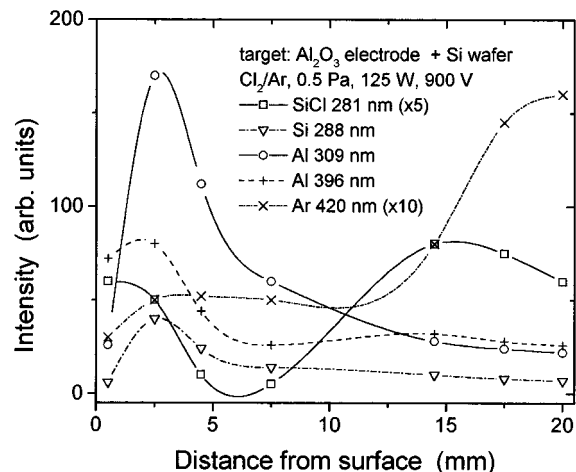
nm. The detection system was mounted on a movable platform. Spatial distributions of the plasma emission were measured by scanning of the platform in the vertical direction with precision better than 1 mm. For measurements with higher spectral resolution a large 0.6-m monochromator (spectral resolution of about 0.2 nm) was employed.

III. EXPERIMENTAL RESULTS

A large number of species were identified in the emission spectra including the main plasma species (Ar, Cl_2, Cl_2^+, Cl, O_2^+, O, etc.) and various etch products or their fragments (Si, Al, Ga, SiCl, AlCl, etc.).[20] The measured spatial distributions of light emission from the main plasma species and those originated from the processed material were found to be essentially different. Some examples of distributions observed at different plasma conditions are presented in Figs. 2–6. The light emission of the species like Si, Al, and SiCl coming from the processed material is strongly localized near the target surface, typically, within several millimeters. For most cases, maximum intensities were detected not exactly at the target surface as expected,[10,11] but at some distance (typically, 2–3 mm) above it. The emission by the main plasma species in the sheath is, typically, several times less than in the bulk plasma and decreases rapidly at the plasma–sheath boundary.

The SiCl molecular emission (near 281 nm) close to the Si target was observed for chlorine-containing plasmas (Cl_2 and $SiCl_4$). In $SiCl_4$ discharges (Fig. 3), the SiCl emission was stronger in the bulk plasma, decreasing towards the electrode. A similar behavior was observed for the $SiCl_2$ emission [continuum at 330 nm (Refs. 20 and 22)] indicating the same origin of excited SiCl and $SiCl_2$ molecules in this case (most probably, electron impact dissociation of $SiCl_4$). The Si atom line emission shows the essentially different spatial profile, with a sharp peak near the surface followed by a fast decay. The intensity ratio for several selected Si lines (221, 251, and 288 nm) changes with distance from the surface and
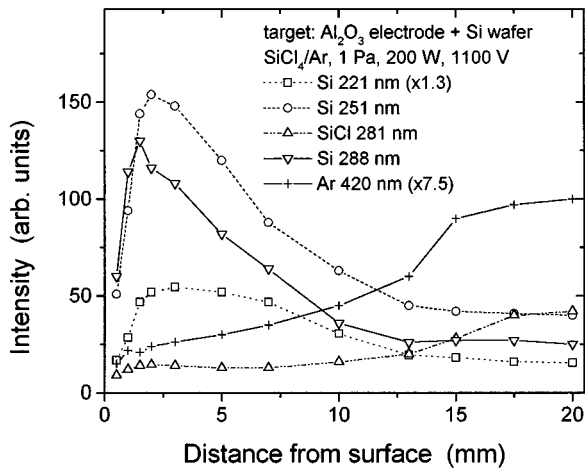
FIG. 3. Spatial distribution of emission in the sheath region, $SiCl_4/Ar=10/10$ sccm, 200 W, 1 Pa, and $E_i \approx e U_{sb} \approx 1100$ eV. Sheath thickness ≈ 15 mm. Other conditions are the same as for Fig. 2.

FIG. 5. Spatial distribution of emission, $O_2/Ar=45/4.5$ sccm, 50 W, 0.5 Pa, and $E_i \approx e U_{sb} \approx 420$ eV. Target: Al_2O_3 electrode. Sheath thickness ≈ 20 mm. Interelectrode gap 5 cm. Other conditions are the same as for Fig. 2.

only in the bulk plasma becomes constant. This clearly shows that the origin of the Si atom emission in the main plasma and near the electrode is different. In the main plasma under the present low-density, low-pressure conditions, direct excitation from the ground state by electron impact is the basic mechanism of formation of the observed excited atomic states, with minor contribution from other processes (like dissociative excitation or cascading from higher levels[4]). In contrast, the near-surface optical emission from sputtered target atoms involves essentially cascading from highly excited atomic levels (see Sec. IV B). In Cl_2 discharges (Fig. 2), the emission by Si atoms is much stronger in the sheath than in the bulk plasma. The decay of the SiCl emission with distance from the surface in this case (Cl_2 plasma) is always faster than that of Si atoms. It is necessary to note that while in the bulk plasma (both for Cl_2 and $SiCl_4$ discharges) SiCl molecules were found to emit basically at

280.9 and 282.3 nm ($B'^2\Delta \rightarrow X \,^2\Pi_r$ transition[23,24]), near the electrode (within 1–2 mm) the spectral maximum of emission was shifted to 280 nm with the smaller peak appearing at 285 nm. This is likely due to rotational (and vibrational) excitation of molecules during their sputtering from the surface. The detailed consideration of this effect is presented elsewhere.[25] Strong rotational and vibrational excitation of such molecules was reported in several works.[26–29]

For the study of emission spectra in GaAs/Cl_2 RIE experiments, enhanced spectral resolution was needed because of the small sizes of the samples (≤ 1 cm^2) utilized. Measurements performed using the large monochromator (with a spatial resolution of 3 mm) show that the Ga atom emission (basically, a strong Ga 417 nm line) also has maximum intensity near the target surface.

The light signals emitted by various species were measured as a function of rf power (the self-bias potential) both

FIG. 4. Spatial distribution of emission in the sheath region, O_2, 45 sccm, 125 W, 1 Pa, $E_i \approx e U_{sb} \approx 700$ eV. Sheath thickness ≈ 20 mm. Other conditions are the same as for Fig. 2.
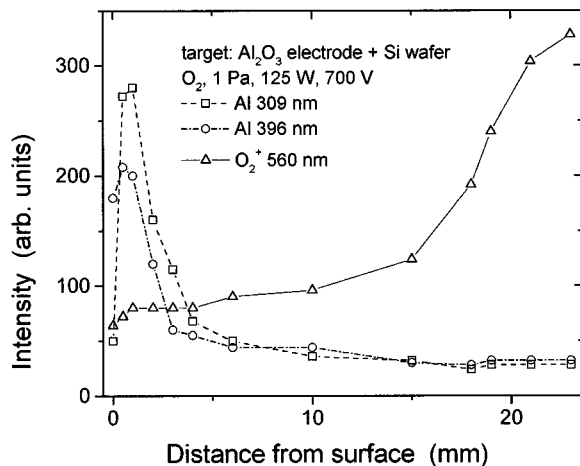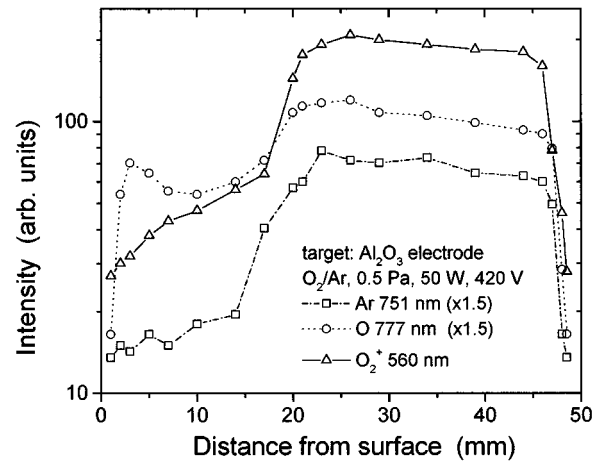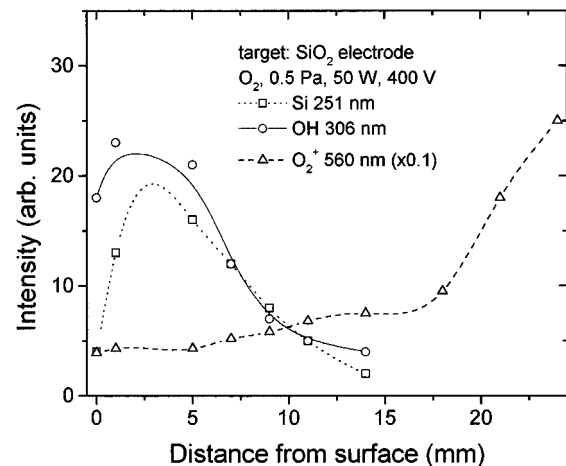

FIG. 6. Spatial distribution of emission in the sheath region, O_2, 45 sccm, 50 W, 0.5 Pa, and $E_i \approx U_{sb} \approx 400$ eV. Target: SiO_2 electrode. Sheath thickness ≈ 23 mm. Other conditions are the same as for Fig. 2.

TABLE I. Dependence of emission intensities (arb. units) in the sheath and in the bulk plasma on rf power (self-bias potential). Emission was collected from the regions centered at ~ 2 mm (sh.) and ~ 20 mm (pl.) above the target, respectively, with a spatial resolution of 3 mm. Process conditions: $Cl_2/Ar=6/1.5$ sccm, and gas pressure 0.5 Pa. Target: Al_2O_3 electrode+Si wafer+GaAs sample ($S_{GaAs}=1$ cm^2).

P, W	U_{sb}, V	Si 251 nm		SiCl 281 nm		Al 396 nm	AlCl 261 nm	Ga 417 nm		GaCl 338 nm		Ar 419 nm		Cl$_2$ 256 nm	Cl$_2^+$ 449 nm	
		sh.	pl.	sh.	pl.	sh.	sh.	sh.	pl.	sh.	pl.	sh.	pl.	pl.	sh.	pl.
20	180	0.35	2.5	0.2	1.0	3.1	1.1	2.5	7.0	1.3	5.0	2.0	8.5	5.0	0.8	3.3
50	420	1.2	7.9	1.8	3.4	5.8	1.5	4.5	26	2.3	12	3.3	10	8.5	1.2	4.3
80	600	1.9	8.7	4.8	4.3	12	3.0	12	28	5.6	16	2.3	12	6.0	0.9	2.8
125	900	2.8	11	10	5.0	32	8.5	⋯	⋯	⋯	⋯	2.7	12	5.0	0.5	2.1

for the sheath (near the electrode) and the bulk plasma regions (Table I). The dependencies obtained are essentially different for the emission of the main plasma species and for the near-surface emission by particles ejected from the target. The GaAs etch rate and the near-surface Ga atom emission also show the different behavior with rf power (Fig. 7). At a high chlorine content in Cl_2/Ar gas mixtures (50%–80%), a square etch rate dependence was observed for rf power up to 50 W. With further power rise [the dashed part of curve 1, Fig. 7(a)], the GaAs etch rate dropped off. The fall of the etch rate with power $P>50$ W is due to the high flux of easily ionized impurities (the etch products from the processed material) to the plasma, which cause a substantial cooling of plasma electrons.[20] The corresponding drop of the light signals from the main plasma species like Cl_2 and Cl_2^+ from the bulk plasma can be seen in Table I. The Ga line emission from the bulk plasma also shows correlation with the GaAs etch rate, with the tendency to saturate at $P \geq 50$ W. At the same time, a fast rise of the Ga emission near the target surface is observed [Fig. 7(b)]. A fast rise of the near-surface optical emission intensity with the self-bias potential (typically, faster than linear) was observed for all particles originated from the target materials (Table I). At a low chlorine content, with a reduced flux of etch products to the plasma, the effect of plasma cooling by impurities was eliminated. As the chlorine content in the gas mixture decreases, the etch rate dependence on power changes from square to linear [Fig. 7(a)].

In O_2 discharges, local maximums near the electrode surface were observed for light emission by O atoms (Fig. 5) and OH molecules [$A\ ^2\Sigma \rightarrow X\ ^2\Pi$ transition, with a larger peak at 306 nm and a smaller one at 281 nm (Refs. 23 and 30)]. Excited OH molecules likely originate from water molecules adsorbed on the electrode surface. The near-surface OH emission was detected both for Al_2O_3 and SiO_2 electrodes. Figure 6 shows a spatial distribution of emission near the SiO_2 electrode.

The experiments carried out with varying gas flow rate show that while the emission by the main plasma components (as well as that of etch products in the bulk plasma) is considerably affected by the flow rate, the near-surface light emission from sputtered particles changes only slightly. As

the chlorine content increases, the emission from sputtered excited particles in the vicinity of the electrode rises (Table II), indicating that their excitation yields depend essentially on the surface coverage.
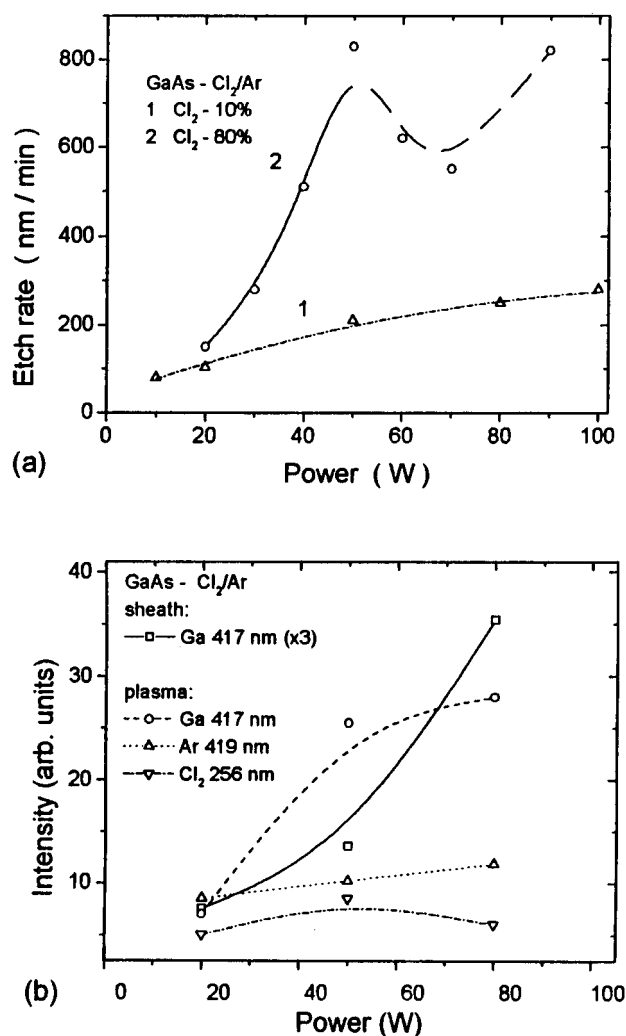

FIG. 7. Data on the GaAs RIE in Cl_2/Ar, total pressure 1 Pa. (a) GaAs etch rate vs discharge power; 1, $Cl_2/Ar=1/9$ sccm; and 2, $Cl_2/Ar=32/8$ sccm. (b) Emission intensities vs discharge power, $Cl_2/Ar=32/8$ sccm. Emission was collected from the regions centered at ~ 2 mm (sheath) and ~ 20 mm (plasma) above the target, respectively, with spatial resolution of 3 mm.

TABLE II. Dependence of emission intensities (arb. units) in the sheath on chlorine content in Cl_2/Ar gas mixture. Emission was collected from the region centered at ~ 2 mm above the target, with a spatial resolution of 3 mm. Process conditions: total flux 7.5 sccm, rf power 50 W, and gas pressure 0.5 Pa. Target: Al_2O_3 electrode + Si wafer + GaAs sample ($S_{GaAs}=1$ cm^2).

$[Cl_2]/[Cl_2+Ar]$, %	U_{sb}, V	Si 251 nm	SiCl 281 nm	Al 396 nm	AlCl 261 nm	Ga 417 nm	GaCl 338 nm
20	480	0.6	0.6	4.6	1.7	1.1	1.5
50	440	1.0	1.4	5.1	1.5	3.0	2.2
80	400	1.2	1.8	5.8	1.5	4.5	2.3

IV. DISCUSSION

A. Origin of secondary photon emission

The effect of a secondary photon emission induced by ion impact is well known from beam sputtering experiments.[7–13] In that case, electronically excited particles are produced during sputtering by energetic ions bombarding a target. In plasma experiments, this kind of emission localized near electrode surfaces was reported in a few works.[14–17,31] In addition to excitation during sputtering, several other possible mechanisms were discussed including: (i) excitation resulting from backscattering (fragmentation as well) of incident ions upon collisions with the surface;[31] (ii) excitation by secondary electrons emitted from the surface under irradiation by energetic ions or photons,[14,32] and subsequently, accelerated by the sheath potential; and (iii) thermalization of sputtered atoms due to elastic scattering on molecules of an ambient gas followed by excitation by plasma electrons.[14] However, these mechanisms are likely of little importance under the present conditions. Contribution of excitation during backscattering (fragmentation) was shown to be sufficient only at relatively low ion energies (less than 100 eV).[31] Excitation by secondary electrons should result also in enhancement of light emission from the main plasma species like Cl_2 and Ar, however, no local peaks were observed for them (see, for example, Figs. 2, 3, and 5). Finally, thermalization of sputtered atoms, which may be important at higher pressures, should result in essentially broad distributions of the near-surface light emission, in contrast to that observed (e.g., Figs. 2 and 3).

Excitation of sputtered atoms during ion bombardment was studied basically for the case of metal sputtering in beam experiments.[7–11] It was shown that only a small fraction of the faster atoms can leave the surface excited. The probability that an atom in the j-excited level will not undergo one of the possible radiationless deexcitation electron exchange processes with the solid surface (resonance ionization, Auger deexcitation), is given by the so-called survival factor:[7]

$$P^j_{surv}=\exp(-A^j/v_m), \qquad (1)$$

$$v_m=[(2E_1/M_2)4M_1M_2/(M_1+M_2)^2]^{0.5}, \qquad (2)$$

where v_m is the maximum velocity that can be obtained by a target atom of mass M_2 in a collision with an ion of mass M_1 and energy E_1, and the parameter A^j is in the order of 10^7 cm/s. Most of the sputtered atoms produced during a collisional cascade in the substrate material have energies of several eV, which correspond to the velocities of $2-5 \times 10^5$ cm/s. Hence, the majority of sputtered atoms (i.e., the slow ones, produced in a collision cascade) may undergo the deexcitation electron exchange process with the solid surface. The faster atoms can be produced only in the first few collisions of the ion with the target atoms. The excitation yield Y^* for sputtered atoms is known to be strongly dependent on surface conditions. Oxygen coverage usually enhances the excitation yield. The pronounced effect of oxygen (as well as nitrogen) coverage was reported in Ref. 7 for sputtering of Be. In the case of GaAs sputtering by a 10 keV Ar^+ beam,[13] the intensity of the secondary Ga atom emission was found to be in proportion to the oxygen coverage. This phenomenon was attributed to the formation of oxide transient molecules in the surface, which can dissociate during sputtering and produce excited atoms through the process of level crossing. Thus, we can consider the parameter A^j in Eq. (1) as surface coverage dependent.

A distribution of excited levels population for fast sputtered atoms generally is not known. In beam experiments, population of highly excited levels of sputtered atoms is commonly assumed to decrease rapidly with the level energy.[9] The initial population of excited levels can be described in terms of the effective excitation temperature, which depends on the incident ion energy and can be estimated to be as small as 0.1–0.5 eV for ion energies as large as 10–80 keV.[9] However, in a collisionless environment (the density of ions in a beam is very low), relaxation of highly excited levels can be realized only through the radiative decay, which is very slow for long-wavelength transitions.[14] Therefore, the initial excitation of high levels is unlikely to affect the observed secondary photon emission in beam experiments. Thus, the contribution of a cascade feeding from high- to low-lying levels is generally not considered.[7] This is also justified by the fact that the measured spatial distributions of secondary emission intensity, typically, show a simple exponential (monotonical) decay with distance from the surface given by a simple expression $I^*(x) \sim \exp(-x/\Delta)$, where x is the distance from the surface, $\Delta = v_\perp \tau$ is the emission decay length, $v_\perp$ is the atom velocity component normal to the surface, and τ is the excited level lifetime.[8,10,11] Note that even for relatively high ion energies (~ 10 keV) the measured decay lengths were as small as 1–2 mm,[8,10–12] whereas in our experiments at much lower ion energies (≤ 1 keV) the higher values of decay lengths (typi-
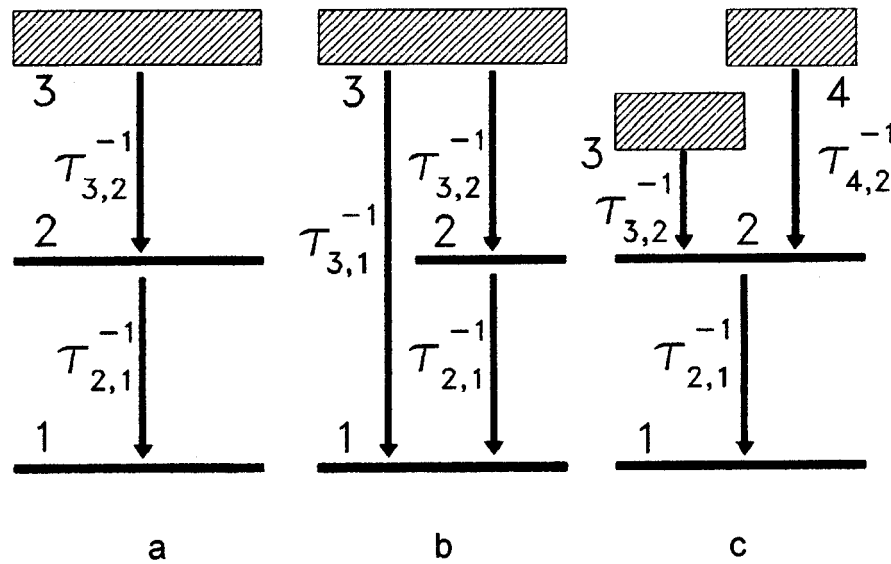
FIG. 8. Simplified schemes of the atomic levels contributing to the observed transition $2 \rightarrow 1$; a, higher levels decay only to level 2; b, higher levels decay both to levels 2 and 1; and c, two groups of higher levels (3 and 4) decay to level 2 with different rates.

cally, 3–4 mm) were observed. Besides, in our case the maximum emission is observed at some distance above the surface (see, for example, Figs. 2, 3, and 6). These facts give evidence that under the present conditions efficient excitation of many upper-lying atom levels during sputtering takes place, so that cascade repopulation (feeding) from high- to low-lying levels should be taken into account.

In a reactive plasma environment, the process of surface sputtering by energetic ions has several distinctive features. First, the surface is normally covered by chemisorbed radicals, which form a top layer rich in intermediate etch products weakly bound to the surface. Ion bombardment results in chemically enhanced sputtering, which is known to be much more efficient than physical sputtering. Besides, one can suppose that the atomic excitation yield can also be strongly enhanced under high coverage conditions since a large part of atoms sputtered from the surface top layer may be previously in a molecular form. Second, under plasma conditions the population of excited levels of sputtered atoms can be perturbed by electric fields and collisions in the sheath region, causing enhanced radiationless relaxation of highly excited levels, and eventually, the increased intensity of the observed emission.

B. Model of cascade feeding

In order to estimate the effect of cascading, a simplified scheme of levels can be considered. In this scheme, the upper levels are grouped into one or two levels decaying with some average relaxation rate through the lower ones. Several possible three- and four-level schemes are depicted in Fig. 8, where 1 and 2 are the lower and upper levels of the observed transition, $\tau_{i,k}^{-1}$ are the rates of decay from i to k level, and $\tau_{2,1}^{-1} \gg \tau_{3,2}^{-1}, \tau_{4,2}^{-1}$. In this consideration, the initial population ($t = 0$) of level 2 will be neglected in comparison with subsequent repopulation from the higher levels 3 and 4, i.e.,

$N_2(0) \ll N_3(0), N_4(0)$. Starting from the population equations for the levels under consideration (in particular, for the case a, these equations can be written as: $dN_3/dt = -N_3/\tau_{3,2}$, $dN_2/dt = N_3/\tau_{3,2} - N_2/\tau_{2,1}$, and $\Sigma N_k(t) = N_3(0)$, where N_k is the population of the k level), one can readily obtain the following solutions for $N_2(t)$ in the three-level scheme (cases a and b, Fig. 8):

$$N_2(t) = \frac{N_3(0)\tau_{2,1}}{\tau_3 - \tau_{2,1}}\left[\exp\left(-\frac{t}{\tau_3}\right) - \exp\left(-\frac{t}{\tau_{2,1}}\right)\right], \quad (3)$$

where τ_3 is the effective lifetime of level 3, which is equal to (i) $\tau_{3,2}$, for case a, or (ii) $\tau_{3,2}\tau_{3,1}/(\tau_{3,2} + \tau_{3,1})$ (i.e., determined by the smallest of the times $\tau_{3,1}$ and $\tau_{3,2}$), for case b. For case c, the solution can be obtained by summing of expressions like that in the right side of Eq. (3) over two distinguished channels of feeding: $N_2(t) = \Sigma_{i,k=4,3}N_{k \rightarrow 2}(t)$, with the relative contribution of the feeding rate from the k to level 2 determined by the term $N_k(0)/\tau_{k,2}$. In Eq. (3), the initial population of level 2 can be taken into account by adding the term $N_2(0)\exp(-t/\tau_{2,1})$. From the solution for $N_2(t)$, the temporal dependence of the observed $2 \rightarrow 1$ transition intensity can be obtained: $I^*(t) \propto N_2(t)/\tau_{2,1}$, as well as the corresponding spatial emission profile $I^*(x)$, where $x = v_{\perp}t$. Here, we ignore the angular distribution of the excited sputtered atoms, (i.e., $v \approx v_{\perp}$), since the survival factor decreases rapidly with ejection angle β as $\exp(-A^j/v_m \cos\beta)$. The solutions obtained show a nonmonotonical behavior of the emission in time (and in space), with a fast rise followed by a slow decay (with the time scales $\tau_{2,1}$ and τ_3, respectively) like that observed in our experiments (e.g., Fig. 3). Note that now (the plasma environment) the emission decay length is determined mostly by the value of τ_3, the effective lifetime of level 3, i.e., $\Delta_p = v_{\perp}\tau_3$. The

TABLE III. Velocities and kinetic energies of excited sputtered atoms in various plasma conditions as derived using Eqs. (3) and (4).

Gas	Target	Pressure, Pa	P, W	U_{sb}, V	$v_{\perp}$, 10^6 cm/s	E_{kin}, eV
O_2	Al_2O_3	1.0	125	700	2.8 (Al)	110
	Al_2O_3	1.0	50	440	2.0 (Al)	55
O_2/Ar	Al_2O_3	0.5	50	420	3.0 (O)	75
Cl_2/Ar	Al_2O_3	0.5	125	900	6.0 (Al)	500
	Si				7.0 (Si)	730
	Si	0.5	50	420	3.0 (Si)	130
$SiCl_4$/Ar	Al_2O_3	1.0	200	1100	4.5 (Al)	280
	Si				7.0 (Si)	730

value of Δ_p can be obtained from the logarithmic plot of the emission intensity profile $I^*(x)$. The time (and position) of peak emission by the $2\rightarrow1$ transition can be found from the condition $dN_3/dt=0$ as

$$t_{peak}=\frac{x_{peak}}{v_{\perp}}\approx\frac{\tau_{2,1}\tau_3}{\tau_3-\tau_{2,1}}\ln\frac{\tau_3}{\tau_{2,1}}. \qquad (4)$$

The ratio x_{peak}/Δ_p depends only on the parameter $K=\tau_3/\tau_{2,1}$ and does not depend on $v_{\perp}:x_{peak}/\Delta_p=\ln K/(K-1)$. Thus, from the measured x_{peak}/Δ_p, the values of K and τ_3 can be determined, if $\tau_{2,1}$ is known. Finally, from the Δ_p value the mean velocity of sputtered excited atoms $v_{\perp}$ can be estimated. Using this approach, the experimental data on emission spatial distributions were analyzed. Data on excited level lifetimes from Ref. 33 were used. For example, in the case of Cl_2 discharge (rf power $P=125$ W, $U_{sb}\approx900$ V), for sputtered excited Al atoms (Al 309 nm line, $\tau_{2,1}=1.4\times10^{-8}$ s) from the measured values of $x_{peak}\approx2$ mm and $\Delta_p\approx6$ mm, the following values were derived: $K\approx7$, $\tau_3\approx10^{-7}$ s, and $v_{\perp}\approx6\times10^6$ cm/s ($E_{kin}\approx500$ eV). The derived values of velocities and kinetic energies of excited sputtered atoms for various discharge conditions are presented in Table III. The velocities obtained are in the range of $2-7\times10^6$ cm/s. The corresponding kinetic energies range from 50 to 700 eV; they are comparable with the kinetic energies of ions bombarding the target (which are approximately equal to the self-bias potential, i.e., $E_i\approx eU_{sb}$). Note that for O_2 plasma, the observed near-surface oxygen atom emission may be due to both backscattering of molecular ions O_2^+ (followed by their neutralization and dissociation) and sputtering of chemisorbed oxygen.

Unlike atoms, excited sputtered molecules do not show clear evidence of a cascade feeding from the upper electronic states, since a monotonical decay with distance from the target surface is typically observed for molecular secondary photon emission (for example, the SiCl emission in Fig. 2). For the near-surface SiCl emission (Cl_2 discharge) the measured decay length slightly exceeds 1 mm, i.e., comparable with the present measurement accuracy. In this case, only the upper limit for a molecular velocity can be estimated. It gives the value of $v_{\perp}\leq1.5\times10^5$ cm/s ($E_{kin}\leq1$ eV) if the emitting state is $B'^2\Delta$ whose lifetime is 1 μs.[34] If the emitting state is a nearly isoenergetic $B^2\Sigma^+$ (the lifetime is 10 ns), the emission decay length should be much less than 1
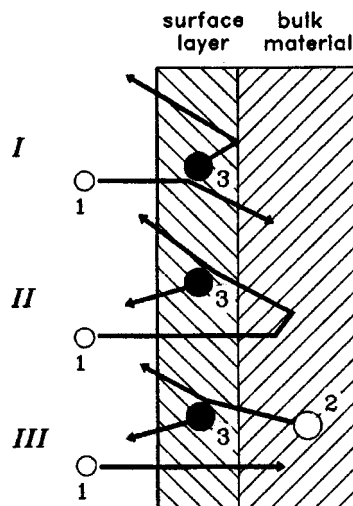

FIG. 9. Main mechanisms involved in ion-induced sputtering of surface adsorbates (adapted from Ref. 35).

mm. For excited sputtered OH molecules, the measured emission decay length is about 4 mm (O_2 discharge, $U_{sb}=450$ V, Fig. 6). Since the upper $A\ ^2\Sigma$ state lifetime is 0.7 μs,[30] this corresponds to $v_{\perp}\approx5\times10^5$ cm/s and $E_{kin}\approx2$ eV. This is in agreement with the data from the beam experiment,[26] where small kinetic energies of 2–3 eV were found for SiH and SiN sputtered excited molecules, without significant variations with kinetic energy of incident ions ($E_i>1$ keV). Therefore, the origin of excited sputtered molecules is evidently different from that of atoms (most probably, a knock-off by slow secondary target atoms produced during a collision cascade of the primary ion in the target). Collisions with fast ions likely cause dissociation of surface molecules rather than their internal excitation.[25,28]

C. Excitation yields

Following Winters and Sigmund,[35] we can distinguish three main mechanisms that dominate the ion-induced sputtering of surface adsorbates (Fig. 9):

(I) Direct knock-off contribution due to direct transfer of energy from the incident ion (1) to the surface atom (3), this mechanism is less effective in the case of normal incidence.

(II) Reflected ion contribution, sputtering by the primary ion (1), reflected from the lattice atoms (2) after the first few collisions.

(III) Sputtered atom contribution due to the outward secondary flux of target atoms (2) caused by the energetic primary ion through the collisional cascade, which can subsequently knock off a surface atom or molecule (3).

Let us consider possible contributions of these mechanisms to the excitation yield of sputtered particles. Through mechanisms I and II, fast recoil atoms are produced with energies comparable with those of incident ions (roughly, in the range of $10-10^2$ eV), and a certain part of them can be

excited [see Eq. (1)]. Mechanism III is responsible for ejection of slow recoil atoms and molecules. Secondary target atoms produced in a collision cascade have energies of several eV. This is enough to eject weakly bound surface-layer molecules without dissociation, with a large fraction of them being excited.[28,36,37] The energy distribution of sputtered target atoms is known to depend only slightly on the energy of primary ions E_i,[38] thus, the excitation yield for recoil molecules can be assumed to be dependent on E_i basically as $S_{III}(E_i)$ in the energy range of interest. Taking into account the different origin of excited atoms and molecules, we can write the ion energy dependences of excitation yields, as follows:

$$Y_{at}^*(E_i) \propto J_i[S_I(E_i) + S_{II}(E_i)]P_{surv}^\Sigma, \tag{5}$$

$$Y_{mol}^*(E_i) \propto J_i S_{III}(E_i)\theta, \tag{6}$$

where J_i is the ion flux to the surface, S_I and S_{II} are the sputtering yields for fast recoil atoms (mechanisms I and II), S_{III} is the sputtering yield for slow recoil molecules (mechanism III), and θ is the reactant surface coverage. Accounting for the effect of cascading from higher atomic levels, in Eq. (5) we use the generalized definition of the survival factor [the definition given by Eq. (1) is valid for the particular case of negligible cascading]:

$$P_{surv}^\Sigma = \sum \{p_{k,2} \exp[-A^k(\theta)/v_m]\} \Big/ \sum p_{k,2}, \tag{7}$$

where the summation is made over the excited levels k contributing to the observed transition $2 \rightarrow 1$, and $p_{k,2}$ is the probability for an atom initially excited at the level k to relax to the level 2. The parameter A^k is now considered to be dependent on the reactant surface coverage θ (see Sec. IV A). It is consistent with the data presented in Table II, where it can be seen that the increase of chlorine content in the gas mixture (and likely the surface coverage by chlorine) leads to a considerable rise of sputtering-induced atomic optical emission. In Eq. (6) we assume that the surface density of molecules is proportional to θ. It should be noted that if the higher levels have substantially different values of A^k, the resulting $P_{surv}^{(\Sigma)}(v)$ dependence differs from the single exponential curve (Fig. 10). However, if the difference between the particular A^k values does not exceed 30%–40%, it appears that the resulting dependence can be rather well described by a single exponent with $A^\Sigma = \Sigma p_{k,2} A^k / \Sigma p_{k,2}$.

The surface coverage and the rate of material removal (etch rate) in the Cl_2-based RIE process can be found using a simple ion–neutral synergy model based on Langmuir adsorption kinetics.[39,40] In this model, the process is considered as a chemically enhanced ion sputtering, and the etch rate is assumed to be proportional to the incident ion flux and to the surface coverage of the chemically assisting neutral species (spontaneous desorption is neglected). Thus, the etch rate can be expressed in the form [quite similar to Eq. (6)]:

$$R = J_i Y(E_i)\theta/\rho, \tag{8}$$

where $Y(E_i)$ is the chemically enhanced sputtering yield per incident ion and ρ is the target atom density. The steady-state
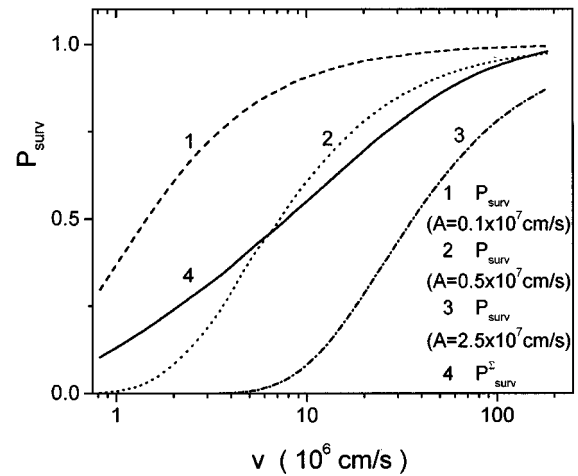

FIG. 10. Dependence of the survival factor on sputtered atom velocity at different values of A^j parameter, calculated using Eq. (1) for curves 1–3 and Eq. (7) for curve 4.

surface coverage θ is determined by a balance between the incoming flux of reactive neutrals and the removal by ion impact. Adsorption onto the surface goes as $(1-\theta)$ as available surface sites become filled: $sJ_n(1-\theta) = \eta J_i \theta$, where J_n is the flux of reactive neutrals to the surface, η is the number of surface sites cleared per ion impact (in other words, the number of reactive neutrals removed from the surface per incident ion), and s is the sticking probability for a reactive neutral arriving at a bare surface. Thus, the surface coverage is given by

$$\theta = (1 + \eta J_i/sJ_n)^{-1}. \tag{9}$$

The value of the sputtering yield $Y(E_i)$ is determined by the composition of partial sputtering yields for the variety of etch products existing at the surface. The dependence of the chemically enhanced sputtering yield on the incident ion energy is given by $Y(E_i) \propto E_i^m$, where m is between 0.5 and 1.[41] So, by measuring of the secondary photon emission intensity as a function of the incident ion energy (self-bias potential), information on the surface coverage can be obtained _in situ_, which then can be used in modeling (and control) of the etch rate, as well as for the study of surface kinetics during plasma processing.

An acceptable agreement (at least, qualitatively) has been found between the model presented and experimental data available for different processing conditions.[16,26,40] In the case of reactive ion-beam etching (RIBE), the relationship between the ion and reactive neutral fluxes to the surface is given by $J_n = qJ_i$, where q is the mean number of halogen atoms in a molecular ion bombarding the substrate. Thus, $\theta = (1 + \eta/sq)^{-1}$, and the dependence of θ on the incident ion energy is dominated by $\eta(E_i)$. Since $\eta \propto E_i$,[39] at low ion energies (where $\eta/sq \ll 1$) the surface coverage is readily saturated ($\theta \approx 1$). With further energy rise the coverage θ begins to fall as E_i^{-1}. Calculations made using the model of sputtering presented in Ref. 35 show that within the ion energy range of interest (0.2–1 keV), the partial yields S_I and

S_{II} decrease slowly and S_{III} increases almost linearly with E_i. Then, from Eqs. (6) and (8) it follows that the etch rate and the molecular excitation yield first rise with E_i, but then tend to saturate at higher ion energies (when $\theta \propto E_i^{-1}$), if J_i is kept constant. Specifically, such a behavior was observed for Al/CCl$_4$ and Si/SiF$_4$ RIBE with saturation of both etch rate and Y_{mol}^* at $E_i > 0.8$ keV,[16] and even the fall of the SiN secondary photon emission was observed at higher ion energies ($E_i > 2$ keV) for Si/N$_2$ RIBE.[26] The dependence of the atomic excitation yield on the incident ion energy is more complicated due to variation of the survival factor, which depends both on E_i and $A^j(\theta)$. Since the parameter A^j is a function of θ, the maximum value of P_{surv}^{Σ} (at the unity level) can be achieved at different values of E_i depending on the surface coverage. With clean surfaces ($A^j > 10^7$ cm/s), the values of E_i exceeding several keV are required for the survival factor to be close to unity. In the case of considerable surface coverage, the effective A^{Σ} value can be several times smaller,[7,13] so that $P_{surv}^{\Sigma} \approx 1$ can be achieved at $E_i \lesssim 1$ keV. Therefore, depending on surface conditions, a different behavior of the atomic excitation yield can be observed including saturation at $E_i > 0.8$ keV (Ref. 16) or monotonical rise[26] with E_i up to several keV.

In contrast to RIBE, where the values of J_i and J_n are of the same order, in the RIE case, typically, the condition $J_i \ll J_n$ is fulfilled (with the only exception for the case of gas mixtures strongly diluted by rare gases, when J_n can be considerably reduced[40]). Then, under RIE conditions the complete surface coverage ($\theta \approx 1$) is readily achieved. For the ion flux to the surface, a linear dependence on the discharge power can be assumed, i.e., $J_i \propto P$. Since $E_i \approx e U_{sb}$, and the self-bias potential U_{sb} rises with power almost linearly (Table I), a square etch rate dependence on power (at $P \lesssim 50$ W) for a high chlorine content in Cl$_2$/Ar [Fig. 7(a)] thus can be explained. Note that the slower rise of the etch rate with power observed for a low chlorine content indicates that a transition to the case $\theta \propto E_i^{-1}$ is realized (as in the RIBE case, see above).

Also, a fast (superlinear) rise with power (i.e., with incident ion energy) was observed both for the molecular and atomic secondary photon emission (Table I). For the latter, a rise of the survival factor with incident ion energy is partially compensated by a slow fall of S_I and S_{II} with E_i. Using the approach developed in Ref. 7, the A^{Σ} value can be estimated by fitting of a theoretical dependence of $Y_{al}^*(E_i)$ given by Eq. (5) to the experimental curves. The estimates of A^{Σ} for several atomic lines were made using the data from Table I and assuming that $E_i = e U_{sb}$. For GaAs/Cl$_2$ RIE under high-coverage conditions [$\theta \approx 1$ (Ref. 40)], the value $A^{\Sigma} \approx 8 \times 10^6$ cm/s was found for the Ga line 417 nm,[25] which is close to that obtained for oxygen-covered Be,[7] and about 1.5 times less than the value found for a clean GaAs surface under Ar$^+$ bombardment.[12] Higher A^{Σ} values ($1.3 - 1.5 \times 10^{-7}$ cm/s) were found for other atomic lines: Si 251 nm and Al 396 nm.[25]

V. CONCLUSION

A portion of the flux of particles sputtered during plasma ion bombardment of a solid surface consists of electronically excited atoms and molecular fragments. These particles are of particular interest because they provide a unique opportunity of *in situ* monitoring of surface processes under plasma exposure. Based on the results of the spatially resolved OES study of atomic and molecular excitation yields, carried out for various plasma conditions, a model of secondary photon emission induced by ion bombardment of the processed surface has been developed. The process of production of excited particles during material sputtering is known from ion beam-sputtering experiments. However, this process in plasmas differs considerably from that in beam sputtering. For atomic secondary photon emission, which demonstrates a nonmonotonical spatial distribution of emission intensity, a cascade feeding from highly excited levels was shown to be important for the plasma case (collisional environment). For molecules, no strong evidence of cascading was found. The origins of excited atoms and molecules were shown to be essentially different. Only a small fraction of fast sputtered atoms (with velocities $2 - 7 \times 10^6$ cm/s) produced in the first few collisions of the incident ion in the target can leave the surface excited. Excited sputtered molecules are knocked off from the surface (with velocities $2 - 5 \times 10^5$ cm/s) by slow secondary atoms produced in a collision cascade of the primary ion inside the solid. The model presented has been shown to be consistent with the experimental data available from different plasma processing experiments (RIE and RIBE). Further experiments are required for the model verification in a wider range of operational conditions.

ACKNOWLEDGMENTS

[1]*Plasma Etching*, edited by D. M. Manos and D. L. Flamm (Academic, Boston, 1988).
[2]A. J. van Roosmalen, J. A. G. Baggerman, and S. J. H. Brader, *Dry Etching for VLSI* (Plenum, New York, 1991).
[3]R. A. Gottscho and T. A. Miller, Pure Appl. Chem. **56**, 189 (1984).
[4]V. M. Donnelly, in *Plasma Diagnostics*, edited by O. Auciello and D. L. Flamm (Academic, New York, 1989), Vol. 1, p. 1.
[5]R. Kelly, Radiat. Eff. **80**, 273 (1984).
[6]W. Berres and H. L. Bay, Appl. Phys. A: Solids Surf. **33**, 235 (1984).
[7]R. B. Wright and D. M. Gruen, J. Chem. Phys. **73**, 664 (1980).
[8]O. Auciello, Phys. Rev. B **24**, 4065 (1981).
[9]R. Kelly, Phys. Rev. B **25**, 700 (1982).
[10]S. Dzioba, O. Auciello, and R. Kelly, Radiat. Eff. **45**, 235 (1980).
[11]S. Dzioba and R. Kelly, Surf. Sci. **100**, 119 (1980).
[12]D. Ghose, Vacuum **46**, 13 (1995).
[13]M. Inoue, Y. Sugiyama, S. Nishigaki, and T. Noda, Nucl. Instrum. Methods Phys. Res. B **33**, 519 (1988).
[14]G. S. Selwyn and E. Kay, Plasma Chem. Plasma Process. **5**, 183 (1985).
[15]R. E. Klinger and J. E. Green, J. Appl. Phys. **54**, 1595 (1983).
[16]S. Dzioba and H. M. Naguib, J. Appl. Phys. **53**, 4389 (1982).
[17]Z. Wronski, J. Sielanko, and J. L. Sullivan, J. Phys. D **29**, 1509 (1996).
[18]R. Kelly, A. Miotello, A. Mele, and A. G. Guidoni, *Experimental Methods in the Physical Sciences* (Academic, San Diego, CA, 1997), Vol. 30, Chap. 5.

[19] R. Kelly, A. Miotello, A. Mele, A. G. Guidoni, J. W. Hastie, P. K. Schenk, and H. Okabe, Appl. Surf. Sci. (submitted).

[20] A. E. Dulkin, V. Z. Pyataev, N. O. Sokolova, S. A. Moshkalyov, A. S. Smirnov, and K. S. Frolov, Vacuum **44**, 913 (1993).

[21] A. E. Dulkin, S. A. Moshkalyov, A. S. Smirnov, and K. S. Frolov, Tech. Phys. **38**, 564 (1993).

[22] D. Sameith, J. P. Mönch, H.-J. Tiller, and K. Schade, Chem. Phys. Lett. **128**, 483 (1986).

[23] R. W. B. Pearse and A. G. Gaydon, *The Identification of Molecular Spectra* (Chapman and Hall, London, 1941).

[24] C. C. Cheng, K. V. Guinn, V. M. Donnelly, and I. P. Herman, J. Vac. Sci. Technol. A **12**, 2630 (1994).

[25] S. A. Moshkalyov, M. Machida, and D. Campos, Jpn. J. Appl. Phys., Part 1 **36**, 209 (1997).

[26] R. Walkup and Ph. Avouris, Surf. Sci. **157**, 193 (1985).

[27] K. J. Snowdon, B. Willerding, and W. Heiland, Nucl. Instrum. Methods Phys. Res. B **14**, 467 (1986).

[28] R. de Jonge, J. Los, and A. E. de Vries, Nucl. Instrum. Methods Phys. Res. B **30**, 159 (1988).

[29] P. G. Fournier, F. Fournier, B. Bellaoui, O. Benoist d'Azy, and G. Taieb, Nucl. Instrum. Methods Phys. Res. B **78**, 144 (1993).

[30] R. Beigang, F. Bozso, Ph. Avouris, and R. Walkup, Nucl. Instrum. Methods Phys. Res. B **13**, 541 (1986).

[31] Y. Yamashita, K. Katayose, H. Toyoda, and H. Sugai, J. Appl. Phys. **68**, 3735 (1990).

[32] R. M. Gilgenbach, C. H. Ching, J. S. Lash, and R. A. Lindley, Phys. Plasmas **1**, 1619 (1994).

[33] *CRC Handbook of Chemistry and Physics*, 72nd ed. (CRC Press, Boston, 1991–1992).

[34] J. B. Jeffries, J. Chem. Phys. **95**, 1628 (1991).

[35] H. F. Winters and P. Sigmund, J. Appl. Phys. **45**, 4760 (1974).

[36] R. Walkup, Ph. Avouris, and D. E. Harrison, Jr., Nucl. Instrum. Methods Phys. Res. B **14**, 461 (1986).

[37] R. Kelly, S. Dzioba, N. H. Tolk, and J. C. Tully, Surf. Sci. **102**, 486 (1981).

[38] M. W. Thomson, Nucl. Instrum. Methods Phys. Res. B **18**, 411 (1987).

[39] A. D. Bailey III, M. C. M. van de Sanden, J. A. Gregus, and R. A. Gottscho, J. Vac. Sci. Technol. B **13**, 92 (1995); *ibid.* **15**, 373 (1997).

[40] S. A. Moshkalyov, M. Machida, S. V. Lebedev, and D. O. Campos, Jpn. J. Appl. Phys., Part 2 **35**, L940 (1996).

[41] C. Steinbrüchel, Appl. Phys. Lett. **55**, 1960 (1989).